Differentiation 90 (2015) 48–58

Contents lists available at ScienceDirect

Differentiation

journal homepage: www.elsevier.com/locate/diff

Immunomodulatory properties and *in vivo* osteogenesis of human dental stem cells from fresh and cryopreserved dental follicles

Young-Hoon Kang [a], Hye-Jin Lee [a], Si-Jung Jang [b], June-Ho Byun [a], Jong-Sil Lee [c], Hee-Chun Lee [d], Won-Uk Park [e], Jin-Ho Lee [f], Gyu-Jin Rho [b], Bong-Wook Park [a,*]

[a] Department of Oral and Maxillofacial Surgery, School of Medicine and Institute of Health Science, Gyeongsang National University, Jinju, Republic of Korea
[b] OBS/Theriogenology and Biotechnology, College of Veterinary Medicine and Research Institute of Life Science, Gyeongsang National University, Jinju, Republic of Korea
[c] Department of Pathology, School of Medicine, Gyeongsang National University, Jinju, Republic of Korea
[d] Department of Medical Imaging, College of Veterinary Medicine, Gyeongsang National University, Jinju, Republic of Korea
[e] Department of Dental Technology, Jinju Health College, Jinju, Republic of Korea
[f] Department of Advanced Materials, College of Life Science and Nano Technology, Hannam University, Daejeon, Republic of Korea

ARTICLE INFO

Article history:
Received 17 April 2015
Received in revised form
9 September 2015
Accepted 9 October 2015
Available online 19 October 2015

Keywords:
Mesenchymal stem cells
Dental follicle cells
Tissue cryopreservation
In vivo osteogenesis
Immunomodulation

ABSTRACT

In our previous study, dental follicle tissues from extracted wisdom teeth were successfully cryopreserved for use as a source of stem cells. The goals of the present study were to investigate the immunomodulatory properties of stem cells from fresh and cryopreserved dental follicles (fDFCs and cDFCs, respectively) and to analyze *in vivo* osteogenesis after transplantation of these DFCs into experimental animals. Third passage fDFCs and cDFCs showed similar expression levels of interferon-γ receptor (CD119) and major histocompatibility complex class I and II (MHC I and MHC II, respectively), with high levels of CD119 and MHC I and nearly no expression of MHC II. Both fresh and cryopreserved human DFCs (hDFCs) were *in vivo* transplanted along with a demineralized bone matrix scaffold into mandibular defects in miniature pigs and subcutaneous tissues of mice. Radiological and histological evaluations of *in vivo* osteogenesis in hDFC-transplanted sites revealed significantly enhanced new bone formation activities compared with those in scaffold-only implanted control sites. Interestingly, at 8 weeks post-hDFC transplantation, the newly generated bones were overgrown compared to the original size of the mandibular defects, and strong expression of osteocalcin and vascular endothelial growth factor were detected in the hDFCs-transplanted tissues of both animals. Immunohistochemical analysis of CD3, CD4, and CD8 in the ectopic bone formation sites of mice showed significantly decreased CD4 expression in DFCs-implanted tissues compared with those in control sites. These findings indicate that hDFCs possess immunomodulatory properties that involved inhibition of the adaptive immune response mediated by CD4 and MHC II, which highlights the usefulness of hDFCs in tissue engineering. In particular, long-term preserved dental follicles could serve as an excellent autologous or allogenic stem cell source for bone tissue regeneration as well as a valuable therapeutic agent for immune diseases.

1. Introduction

Recently, mesenchymal stem cells (MSCs)-based bone tissue engineering techniques have been developed as substitutes for traditional bone grafts in standard procedures for the reconstruction of bone defects. In addition to their effect on the enhancement of bone formation, MSCs possess several advantages for tissue engineering. They can be easily isolated from numerous adult tissues, and thus autologous stem cells can be used without any ethical concerns. Another major advantage of MSCs is their immunomodulatory effects. The immune reactions of MSCs derived from various tissues have been widely studied, and it has been shown that MSCs can regulate T and B lymphocytes, dendritic cells, and natural killer cells (Duffy et al., 2011; Rahimzadeh et al., 2014). This immunomodulatory activity of MSCs allows their use as allogenic transplantation materials and as therapeutic agents for various autoimmune disorders, such as graft-versus-

* Correspondence to: Department of Oral and Maxillofacial Surgery, School of Medicine and Institute of Health Science, Gyeongsang National University, Gangnam-ro 79, Jinju 660-702, Republic of Korea.
E-mail address: parkbw@gnu.ac.kr (B.-W. Park).

http://dx.doi.org/10.1016/j.diff.2015.10.001
Join the International Society for Differentiation (www.isdifferentiation.org)

host disease and systemic lupus (Sui et al., 2013; Zhao et al., 2015). Most studies characterizing the immune response of MSCs have been predominantly focused on bone marrow- or umbilical cord-derived MSCs (BMSCs or UCMSCs) (Chao et al., 2014; Rahimzadeh et al., 2014; Zhuang et al., 2015). However, several recent studies have shown that human MSCs can also be successfully isolated from other adult tissues (Le Blanc and Ringdén, 2006; Park et al., 2014).

Although bone marrow is the most frequently used source of MSCs for tissue engineering studies, dental tissues from extracted wisdom teeth, including dental follicle, pulp, and root apical papilla, were recently shown to be excellent and powerful sources of MSCs for bone regeneration (Park et al., 2012, 2014; Seo et al., 2008; Yamada et al., 2011; Takahashi et al., 2015). Moreover, in our previous report, we showed that the dental follicle tissues of extracted wisdom teeth could be successfully cryopreserved for future use as an autologous stem cell source (Park et al., 2014). We isolated MSC-characterized human dental follicle stem cells (hDFCs) from long-term cryopreserved dental follicle tissues and showed that these cells have similar cell growing morphology and characteristics compared to those derived from fresh dental follicles. In addition, stem cells from cryopreserved human dental follicles (cDFCs) showed the potential to differentiate into mesenchymal lineage cells (osteocytes, adipocytes, and chondrocytes) *in vitro*, similar to MSCs from fresh human dental follicles (fDFCs). However, stability and immunomodulatory activity of cDFCs after *in vivo* transplantation have not yet been investigated.

Therefore, the present study aimed to investigate the immunomodulatory properties of hDFCs from cryopreserved and fresh dental follicles, and to analyze the *in vivo* osteogenic potential of hDFCs after transplantation into experimental animals. In addition, the immunohistochemical (IHC) expression of T cell-related markers (CD3, CD4, and CD8) was analyzed in DFCs-transplanted tissues.

2. Materials and methods

2.1. Chemicals, media, and animal Experimentation approval

All chemicals used in the present study were purchased from Sigma-Aldrich (St. Louis, MO, USA), and all media were from Gibco (Invitrogen, Grand Island, NY, USA), unless otherwise specified. For all media, the pH was adjusted to 7.4 and the osmolality was adjusted to 280 mOsm/kg. All animal experiments using mice and miniature pigs were approved by the Animal Center for Medical Experimentation at Gyeongsang National University.

2.2. Cryopreservation of Human dental follicles and isolation of MSCs

Dental follicle tissues were harvested from extracted wisdom teeth and cryopreserved. MSCs were then isolated from cryopreserved and fresh dental follicles as previously described (Park et al., 2014). Briefly, human dental follicles were harvested from the immature wisdom teeth of 24 patients (12 donors for the tissue cryopreservation group and 12 donors for the fresh tissue group; average age, 18.5 years) extracted at the Department of Oral and Maxillofacial Surgery at Gyeongsang National University Hospital, under approved guidelines (GNUH IRB-2012-09-004-002), and after obtaining informed consent from patients. The dental follicles from 12 donors (6 males and 6 females) were minced into 1–3 mm^2 explants and tissue segments from single donors were put into 1.8 mL cryovials (Thermoscientific, Roskilde, Denmark) containing 1 mL of cryoprotectant (0.05 M glucose, 0.05 M sucrose, and 1.5 M ethylene glycol; osmolality: 1900 mOsm/kg). The cryovials were cryopreserved under a programmed slow freezing protocol as follows: cryovials were equilibrated for 30 min at 1 °C, then cooled at −2 °C/min to −9.0 °C, then cooled from −9.0 °C to −9.1 °C and held for 5 min; then further cooled at −0.3 °C/min to −40 °C; then −10 °C/min to −140 °C. The cryovials were then stored in liquid nitrogen for more than 1 year, after which the cryopreserved dental follicles were thawed by immersion in a circulating water bath at 37 °C for 1 min.

Fresh dental follicles from the other 12 donors (6 males and 6 females) were used for immediate isolation of hDFCs. The isolation and culture of hDFCs from fresh and cryopreserved dental follicles were performed as previously reported (Park et al., 2014). Briefly, dental follicles were digested in D-PBS containing 1 mg/mL collagenase type I at 37 °C for 40 min, and then mechanically dissociated and filtered through a 40 μm cell strainer (BD Falcon, Franklin Lakes, NJ, USA) to obtain single-cell populations. Cells (5×10^5) were cultured in 4 mL of Advanced Dulbecco's Modified Eagle's Medium (A-DMEM) containing 10% fetal bovine serum (FBS) and 1% pen-strep in a 25 T-flask (Nunc™, Roskilde, Denmark) at 37 °C in a humidified atmosphere with 5% CO_2. The medium was changed every 3 days.

2.3. FACS analysis of MHCI and MHCII expression in DFCs

The expression of interferon-γ receptor (IFN-γR, CD119) and major histocompatibility complex class I and II (MHC I and MHC II) proteins was analyzed in passage 3 fDFCs and cDFCs by fluorescence-activated cell sorting (FACS; BD FACSCalibur, Becton Dickson, Franklin Lakes, NJ, USA) analysis in five independent experiments, as previously described (Park et al., 2012, 2014). Briefly, fDFCs and cDFCs were harvested with 0.25% trypsin–EDTA, and then the cells were fixed in a 4% paraformaldehyde solution and incubated in 0.1% Triton X (Sigma-Aldrich) for permeabilization. Primary antibodies for CD119 (1:100; rabbit polyclonal IgG, #sc-25482, Santa Cruz Biotechnology, Inc., Dallas, TX, USA), MHC I (1:100; rabbit polyclonal IgG, #sc-25619, Santa Cruz), and MHC II (1:100; mouse monoclonal IgG, #sc-32247, Santa Cruz) were incubated with both types of DFCs. Fluorescein isothiocyanate (FITC)-conjugated secondary antibodies for CD119, MHC I (1:100; donkey anti-rabbit IgG, #sc-2090, Santa Cruz), and MHC II (1:100; goat anti-mouse IgG, #554001, BD Pharmingen™, BD Bioscience, Franklin Lakes, NJ, USA) were then added for protein detection.

2.4. Bone regeneration by hDFCs in the mandibular defects of miniature pigs

Three male miniature pigs (aged 6–12 months and weighing approximately 25 kg) were used to evaluate *in vivo* bone regeneration in mandibular defects. After sedation and general anesthesia with 4 mg/kg of azaprone (Stresnil®; Janssen Animal Health for Merial Canada Inc., Baie d'Urfe, Quebec, Canada) and 10 mg/kg of tiletamine-zolazepam (Zoletil®, Virbac, Carros, France), as previously described (Kang et al., 2010), the right side of the mandible was exposed by submandibular dissection. Four defects (1.2 cm in diameter and 0.5 cm in depth) were made in the mandibles of experimental animals with a round rotary bur (Fig. 2A). fDFCs or cDFCs (3×10^6) were injected into 0.25 cm^3 of demineralized bone matrix (DBM; SureFuse™ II, HansBiomed Corp., Seoul, Korea) and 0.3 mL of fibrin glue (Greenplast™, Green Cross, Yongin, Korea) scaffold. The mandibular defects were sequentially transplanted with either a no-graft control (No-graft), a scaffold mixture without cells (DBM), scaffold with fDFCs (Fresh+DBM), and scaffold with cDFCs (Cryo+DBM) (Fig. 2A and B). The muscle flap and submandibular skin were closed with 3-0 Vicryl and nylon. A first-generation cephalosporin (Cefazolin, 20 mg/kg for 5 days; Yuhan, Seoul, Korea) and an anti-inflammatory drug (Meloxicam, 2 mg/kg for a day; Boehringer

Ingerheim, Ingelheim, Germany) were injected intramuscularly twice a day. Details, including the animals used, defect size, number of transplanted cells, and the scaffold volume, are summarized in Table 1.

2.5. Ectopic bone formation by hDFCs in the subcutaneous tissues of mice

hDFCs from fresh and cryopreserved dental follicles were transplanted into the subcutaneous tissues of four 8-week-old male BALB/c mice (Charles River, Orient Bio Inc., Sungnam, Korea) to evaluate ectopic bone formation *in vivo*, according to a previously published protocol with minor revisions (Park et al., 2012). Briefly, fDFCs and cDFCs at passage 3 were harvested and labeled with a fluorescent lipophilic carbocyanine dye (PKH26) according to a previously described method (Kang et al., 2010; Park et al., 2012). fDFCs or cDFCs (1×10^6) mixed with 0.2 mL of fibrin glue (Greenplast™) were injected and simultaneously coated in a quarter of a 0.5 cm^3 (0.125 cm^3)-sized DBM (SureFuse™ II) block. A mixture of fDFCs or cDFCs with DBM and fibrin glue scaffold was transplanted under the back skin of four experimental mice. The mice were placed under general anesthesia with a subcutaneous injection of 0.5 μL/g of tiletamine-zolazepam (Zoletil®) and 0.5 μL/g xylazine (Rompun®, Bayer Korea Ltd., Seoul, Korea), and then three small skin incisions (approximately 1 cm each) were made and subcutaneous pouches were formed on the back of each mouse. The scaffold mixtures (fibrin glue and DBM) injected with cDFCs or fDFCs were implanted into the subcutaneous pouches. The control non-cell seeded DBM and fibrin glue scaffold mixture was implanted in the other subcutaneous pouch. After implantation of each mixture, the skin incisions were closed with 4-0 nylon.

2.6. Radiological and histological analysis of in vivo osteogenesis

The experimental mice and miniature pigs were anesthetized at 4 and 8 weeks after transplantation, and the bone formation patterns in each animal were analyzed by plain radiography and computed tomography (CT, SOMATOM Emotion 6, Siemens, Munich, Germany). CT images of the mandibular defects in miniature

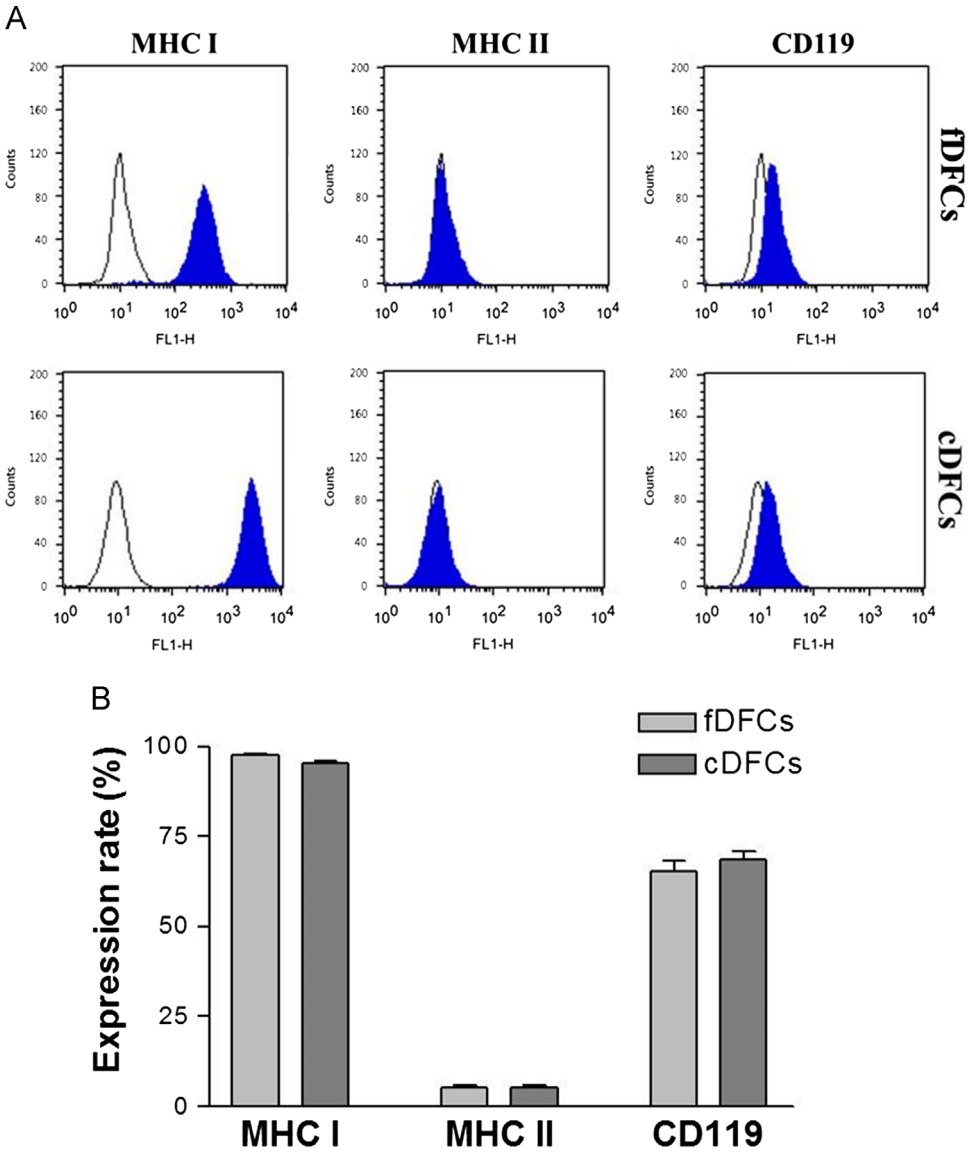

Fig. 1. Fluorescence-activated cell sorting (FACS) analysis of hDFCs derived from fresh and cryopreserved dental follicles. (A) Results of FACS analysis for MHC I, MHC II, and CD119 in fDFCs and cDFCs at passage 3. (B) Statistical analysis of (A) showed similar expression levels of MHC I and CD119 in hDFCs from both fresh and cryopreserved dental follicles, and extremely low MHC II expression. The data represent the mean ± SD of five different experiments.

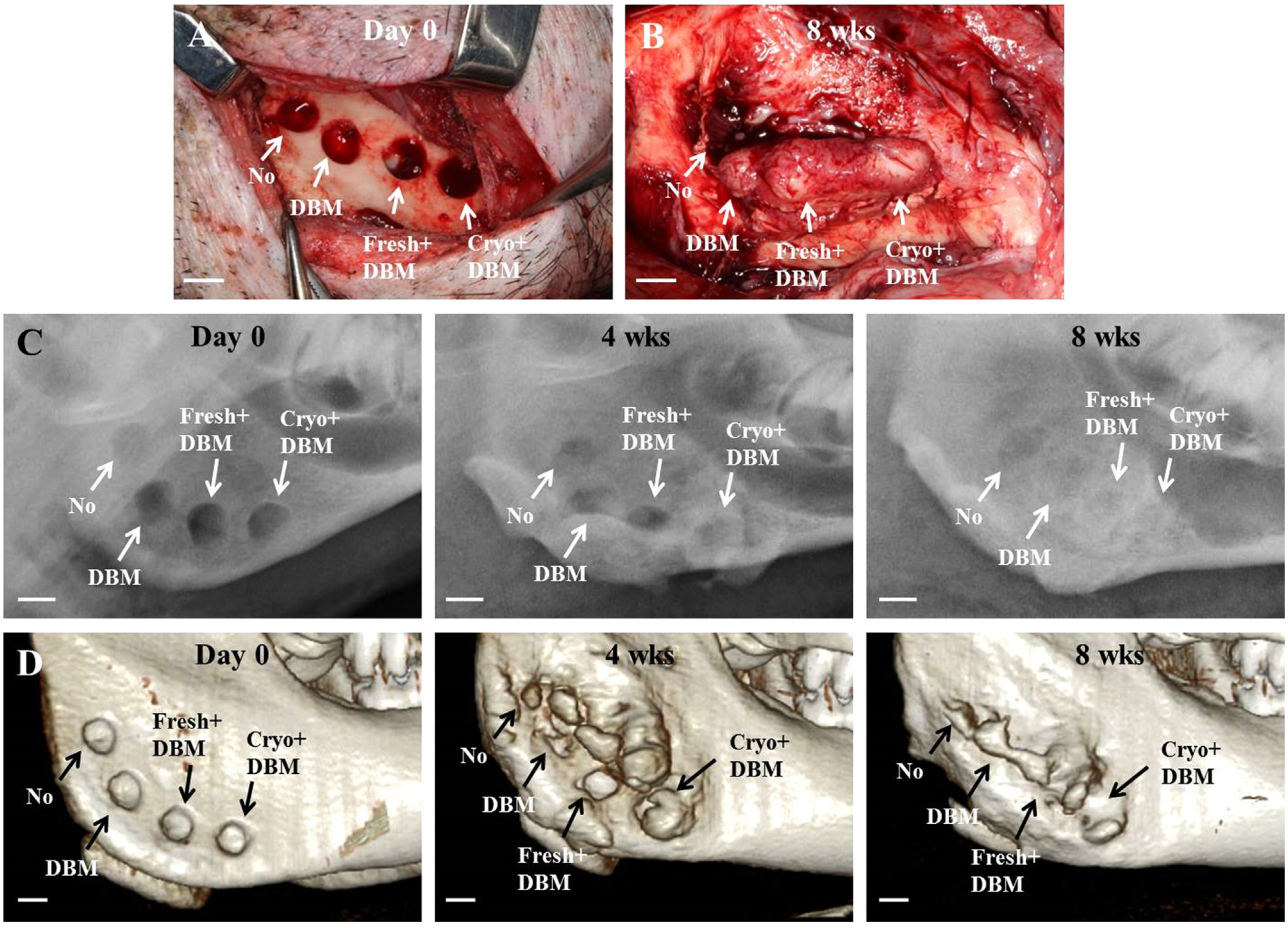

Fig. 2. Representative *in vivo* osteogenesis and radiological images of mandibular defects in miniature pigs (scale bar = 1 cm). (A) Four mandibular defects of the same size (diameter, 1.2 cm and depth, 0.5 cm) were formed in the unilateral mandibular body of animals in four independent transplantation groups: no graft (No), DBM-only graft (DBM), fDFCs and DBM (Fresh + DBM), and cDFCs and DBM (Cryo + DBM). (B) Eight weeks after transplantation, significantly enhanced bone formation and overgrown bony tissue were observed in the hDFC-transplanted groups compared to the control groups, and the fDFC and cDFC showed similar morphology. (C) Radiological evaluation of the mandibular defects shows gradually increasing radio signal intensity in cell-transplanted sites during the observation period. At 8 weeks post-transplantation, complete disappearance of the bony defects and significantly increased radio-opacities relative to those on Day 0 were observed in hDFC-implanted sites. (D) Three dimensional (3D) CT views of miniature pigs showed excessive bone regeneration in the hDFC-transplanted mandibular defects and complete healing of the bony defects at 8 weeks post-implantation.

Table 1
Summary for animal usage, defect number and size, and volume of each transplant.

	Used no. and gender	Age/weight	No. of defects/each defect size	Volume of each transplant	Euthanasia
Miniature pig	3 males	6–12 months/ about 25 Kg	4 mandibular defects/1.2 cm diameter × 0.5 cm depth (=0.565 cm^3)	3×10^6 hDFCs + 0.3 mL Fibrin glue + 0.25 cm^3 DBM	8 weeks
Mice (BALB/c)	4 males	8 weeks/about 25 g	3 subcutaneous pouches/1 cm skin incision and dissection of subcutaneous tissue	1×10^6 hDFCs + 0.2 mL Fibrin glue + 0.125 cm^3 DBM	8 weeks

pigs (4 and 8 weeks post-transplantation) and the ectopic bone formation sites in mice (4 weeks post-implantation) were analyzed and compared with intensity analyzing software (Syngo CT 2004A, Siemens). After obtaining radiographs at 8 weeks post-implantation, all experimental animals were euthanized by KCl injection.

Cell-transplanted subcutaneous tissues were harvested *en bloc* from experimental mice, and the specimens were divided into longitudinal sections for histological and fluorescence analyses. One sectioned specimen from each *in vivo* transplanted site was used for fluorescence detection of PKH26 expression, as previously described (Kang et al., 2010; Park et al., 2012). Briefly, tissues were embedded in optimal cutting temperature compound (Tissue-Tek, Sakura Finetechnical Co., Ltd., Tokyo, Japan), rapidly frozen at −23 °C, and cut into 4 μm sections using a Cryocut (LEICA CM3050S, Leica, Wetzlar, Germany). The sections were mounted on glass slides, and PKH26 expression was assessed using a fluorescence microscope (BX51, Olympus, Tokyo, Japan) equipped with a fluorescent digital camera (DP72, Olympus).

The other specimens from the implant sites of mice were fixed with 10% neutral buffered formalin for 24 h, embedded in a paraffin block, cut into 4 μm sections, and mounted on SuperfrostPlus microscope slides (Fisher Scientific, Rochester, NY, USA). After deparaffinization and hydration, sample sections mounted on glass slides were stained with hematoxylin and eosin (H&E). In addition, sections were prepared for IHC analysis of osteocalcin (OC, an osteogenesis marker), vascular endothelial growth factor (VEGF, an angiogenesis marker), and the T-cell markers CD3, CD4,

Table 2
Information for selected primary antibodies and the results of semi-quantitative analysis for immunostaining intensities in the ectopic bone formations of mice.

Name	Type	Company/ lot no.	Dilution	Immunostaining intensity		
				Con	Fresh	Cryo
CD3	*Rabbit monoclonal*	Lab Vision/ RM-9107	1:1500	+++	++	++
CD4	*Mouse monoclonal*	Thermo Scientific/MS-1528	1:300	+++	+*	+*
CD8	*Rabbit monoclonal*	Thermo Scientific/RM-9116	1:400	+++	+++	+++
OC	*Mouse monoclonal*	Santa Cruz/ sc-390877	1:200	++	+++	+++
VEGF	*Rabbit polyclonal*	Santa Cruz/ sc-152	1:200	++	+++	+++

Abbreviations: CD3, Cluster of differentiation 3; CD4, Cluster of differentiation 4; CD8, Cluster of differentiation 8; OC, Osteocalcin; VEGF, Vascular endothelial growth factor; Con, non-cell implanted control sites; Fresh, fDFC-transplantation sites; Cryo, cDFC-transplantation sites.
Company and location: Lab Vision: Lab Vision Corporation, Fremont, CA, USA; Thermo Scientific: Thermo Fisher Scientific Inc., Fremont, CA, USA; Santa Cruz: Santa Cruz Biotechnology, Inc., Dallas, TX, USA.
* Statistically significant difference compared to control sites ($p < 0.05$).

and CD8 using an automated immunostainer (BenchMark XT, Ventana Medical System Inc., Tucson, AZ, USA), and signals were detected using the Ultraview DAB kit (Ventana Medical System), according to the manufacturer's protocol. Briefly, the mounted specimens were deparaffinized using EZ Prep solution, and then incubated with CC1 standard (pH 8.4 buffer contained Tris/borate/EDTA) for antigen retrieval at 100 °C for 69 min. The slides were incubated with DAB inhibitor (3% H_2O_2) at 37 °C for 4 min to block endogenous peroxidase activity. Next, each primary antibody was added and incubated at 37 °C for 30 min. Then, the secondary antibody, Universal HRP Multimer, was added and incubated at 37 °C for 8 min. Finally, the slides were treated with substrate (DAB+H_2O_2) for 8 min, and then incubated with hematoxylin II and bluing reagent at 37 °C to counter stain nuclei. For the negative controls, the primary antibody was omitted.

IHC staining was semiquantitatively analyzed for antibody deposition in cellular components. Based on a previously reported method with some modification (Watanabe et al., 2014), positive immunostaining for CD3, CD4, and CD8 was scored by a combination of staining intensity (0, negative staining; 1, weak staining; 2, moderate staining; and 3, strong staining) and the proportion of positively stained cells in high-power fields (0, none; 1, < 25%; 2, 25–50%; 3, 51–75%; and 4, > 75%). The sum of the staining intensity and percentage of positive cells scores was graded as follows: +++ (strong, 6–7); ++ (moderate, 4–5); +(weak, 2–3); and − (negative, 0–1). At least four different specimens were used to semiquantitatively assess IHC intensity in hDFC-implanted specimens, and these specimens were statistically compared with control specimens. The primary antibodies used and the IHC staining results are summarized in Table 2.

After euthanizing the experimental miniature pigs by intravenous injection of KCl, the DFCs and/or DBM-transplanted mandibles were segmentally resected using a reciprocating saw, and fixed in 10% neutral buffered formalin for 24 h. They were then decalcified in 5% nitric acid for 3 days. The specimens were embedded in a paraffin block, cut into 4 μm sections, and mounted on slides. Each transplanted specimen was stained with H&E, and a histological analysis of new bone regeneration patterns was conducted. The other specimens of newly generated bone from miniature pigs were also prepared for IHC analysis of OC and VEGF using an automated immunostainer (BenchMark XT), as described above for the mouse specimens.

2.7. Analysis of calcium content in the in vivo ectopic bones of the mice

To measure the calcium contents in the implanted specimens of mice, each sample was deparaffinized, dried at 95 °C for 1 h, weighed, and decalcified in 1 mL of Calci-Clear Rapid (National Diagnostics, Atlanta, GA, USA). The calcium content of the supernatants was determined by spectrophotometry using the Methylxylene blue (MXB) method (Calcium E-test; Wako Pure Chemical Industries, Osaka, Japan) according to the manufacturer's instructions. The calcium level in samples from each group is expressed as the mean ($n=3$) calcium content (in ng) per total specimen (cells and scaffold; in mg).

2.8. Statistical analysis

Independent experiments were repeated at least three times, and the data shown are the mean ± standard deviation (SD). Statistical differences between experimental groups were determined by one-way analysis of variance (ANOVA), followed by Tukey's test for multiple comparisons or an unpaired *t*-test for single comparisons of experimental data relative to the control value using GraphPad Prism. Differences were considered significant at $p < 0.05$, and significant differences are denoted by different letters.

3. Results

3.1. FACS analysis of MHC I and MHC II expression in hDFCs

MHC I and MHC II protein expression was similar in fDFCs and cDFCs. High MHC I expression was observed in both cell types (98.6% and 98.4% in fDFCs and cDFCs, respectively), whereas almost no MHC II expression was detected (4.4% and 3.6% in fDFCs and cDFCs, respectively). In addition, CD119 expression levels in the two types of hDFCs were the same; approximately 65–75% of the hDFCs from fresh or cryopreserved dental follicles was positive for CD119 expression, respectively (Fig. 1).

3.2. Mandibular bone regeneration by hDFCs in miniature pigs

In the hDFC-transplanted mandibular bone defects, remarkably overgrown bone tissues were observed at 8 weeks post-implantation compared with the bone generation in the two control defects (DBM-only and non-graft sites; Fig. 2B). In conventional films at 4 and 8 weeks post-implantation, radiological opacities were markedly higher in the hDFC-transplanted sites than in the DBM-only and non-graft control sites, which showed only weakly increased radiological intensity (Fig. 2C). Three-dimensional (3D) CT showed osteogenesis in the mandibular defects, and remarkably high levels of osteogenesis were detected in the outer layer of defects at 4 weeks post-transplantation. At 8 weeks post-implantation, the defects were completely filled with newly generated bone (Fig. 2D). In the coronal CT views, the non-graft and DBM-only control sites showed progressive osteogenesis within the pre-fabricated mandibular defects. In contrast, the hDFC-transplanted sites showed remarkably enhanced new bone formation (Fig. 3A). Interestingly, this *in vivo* bone formation was overgrown, not only within the bone defect but also within the muscle layers. These intramuscular bone formations fused with the newly generated bone in the pre-fabricated bone defects, leading to excessively overgrown bone formations at 8 weeks

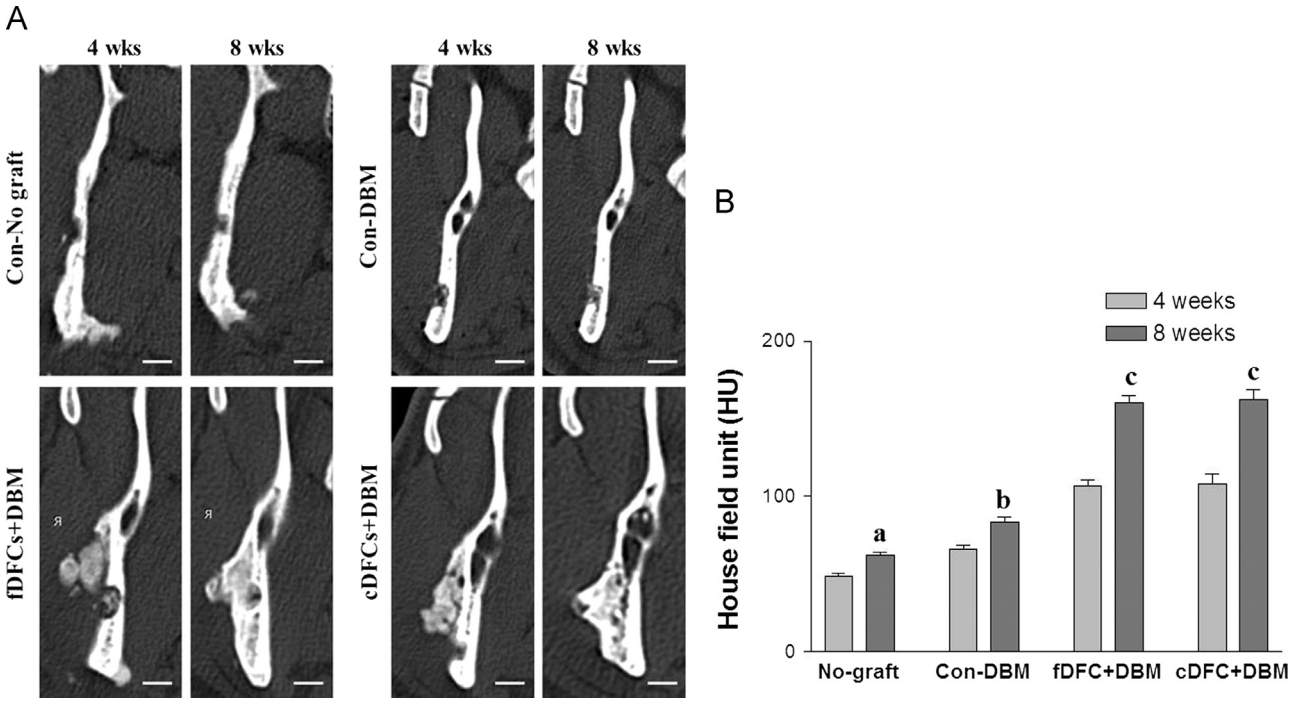

Fig. 3. Computed tomography (CT) and radiological signal intensity analysis of the mandibular defects of miniature pigs (scale bar = 1 cm). (A) Both the fDFC- and cDFC-transplanted sites with DBM scaffold show remarkably increased new bone formation compared to the two control sites (No graft and DBM-only graft). Interestingly, at 4 weeks post-transplantation, new bone formation was observed not only in the bony defect of the mandible but also in the muscle layer surrounding the defects. At 8 weeks post-transplantation, the newly generated bone in the hDFC-transplanted sites covered the bony defects and the hardness was increased. (B) Digitalized radiological signal intensity analysis revealed very similar signal intensities in the fDFC and cDFC groups at 8 weeks post-implantation, and these groups showed remarkably increased radio-opacities compared to those in the two control groups (No graft and DBM-only graft sites). The data represent the mean ± SD of three independent experiments. Different letter subscripts denote statistical differences between groups ($p < 0.05$).

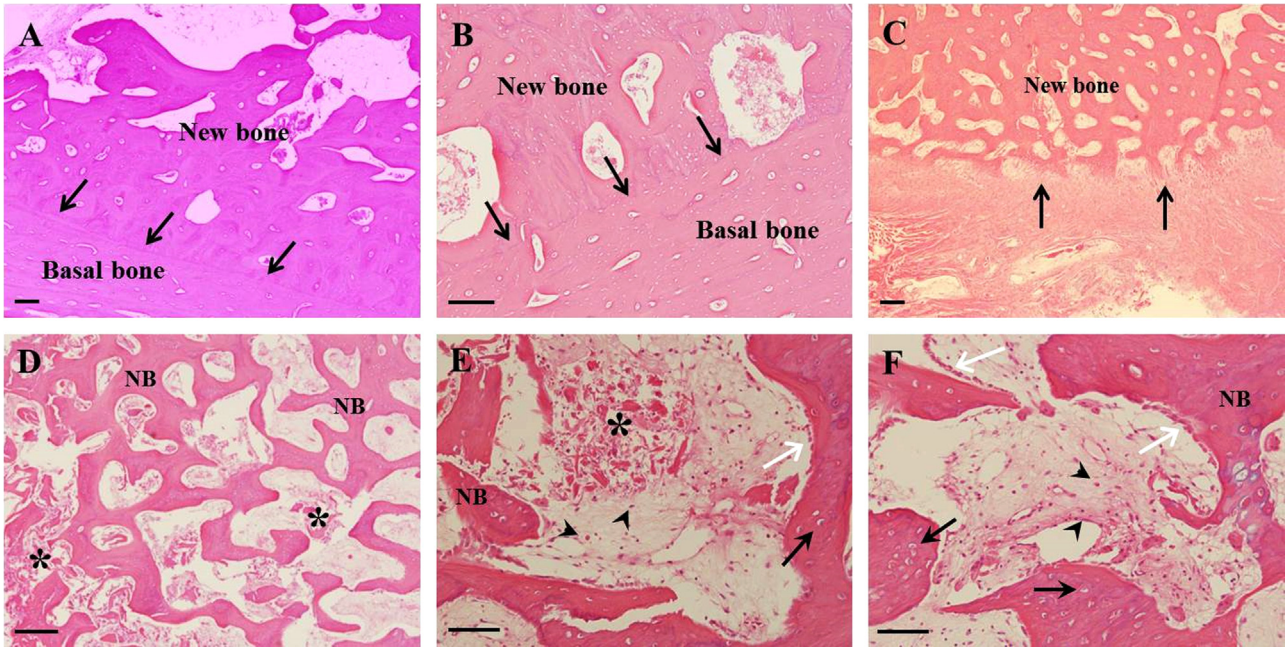

Fig. 4. Histological features of *in vivo* osteogenesis in the mandibular defects of miniature pigs at 8 weeks post-transplantation at sites with hDFCs, DBM, and fibrin glue scaffold (A, B, E: fDFC transplantation; C, D, F: cDFC transplantation; scale bar = 100 μm). Similar *in vivo* new bone formation patterns were observed following transplantation of the two types of hDFCs. (A) Under low magnification, the newly generated bone is discriminated from the basal bone by a borderline (black arrows). (B) Higher magnification of (A) showing the borderline between the basal bone and newly generated bone (black arrows). The new bone near in basal bone showed increased hardness, a lack of bone trabeculae, and its histological appearance seemed to be similar to that of basal bone. (C) Histological features of the newly generated bone on the opposite side of the basal bone. The trabecular bones were continuously generated in the interstitial tissue of transplanted site. (D) Degrading DBM scaffolds (*) were observed in the newly generated bone trabeculae (NB). (E and F) At higher magnification, small particulates of the degrading DBM (*) were detected around the newly generated bone trabeculae (NB). Immature fibroblast-like cells (putative pre-osteoblasts) around new bone matrices (black arrowheads), osteoblasts lining the newly generated trabecular bones (white arrows), and osteocytes trapped in the newly generated bone spicules (black arrows) were abundant in the hDFC-transplanted tissues.

post-transplantation (Fig. 3A). Digitalized radiological intensity analysis showed that there was no difference in the bone formation potential of fDFCs and cDFCs and significantly higher radiological intensity in the DFC-transplanted sites than in the non-cell graft or DBM-only control sites at 8 weeks post-implantation (Fig. 3B).

Histological examination of mandibular specimens at 8 weeks post-implantation revealed that new cortical bone was formed and connected to the basal bone on the inner surface of the graft site (Fig. 4A and B). In the outer portion of the graft site, abundant newly generated trabecular bones were observed with degrading DBM scaffolds (Fig. 4C and D). At higher magnification, enhanced new bone formation was observed in the hDFC-transplanted sites, including immature fibroblast-like cells (putative pre-osteoblasts), lining osteoblasts around the newly generated trabecular bones, and entrapped osteocytes in the new bones (Fig. 4E and F). New

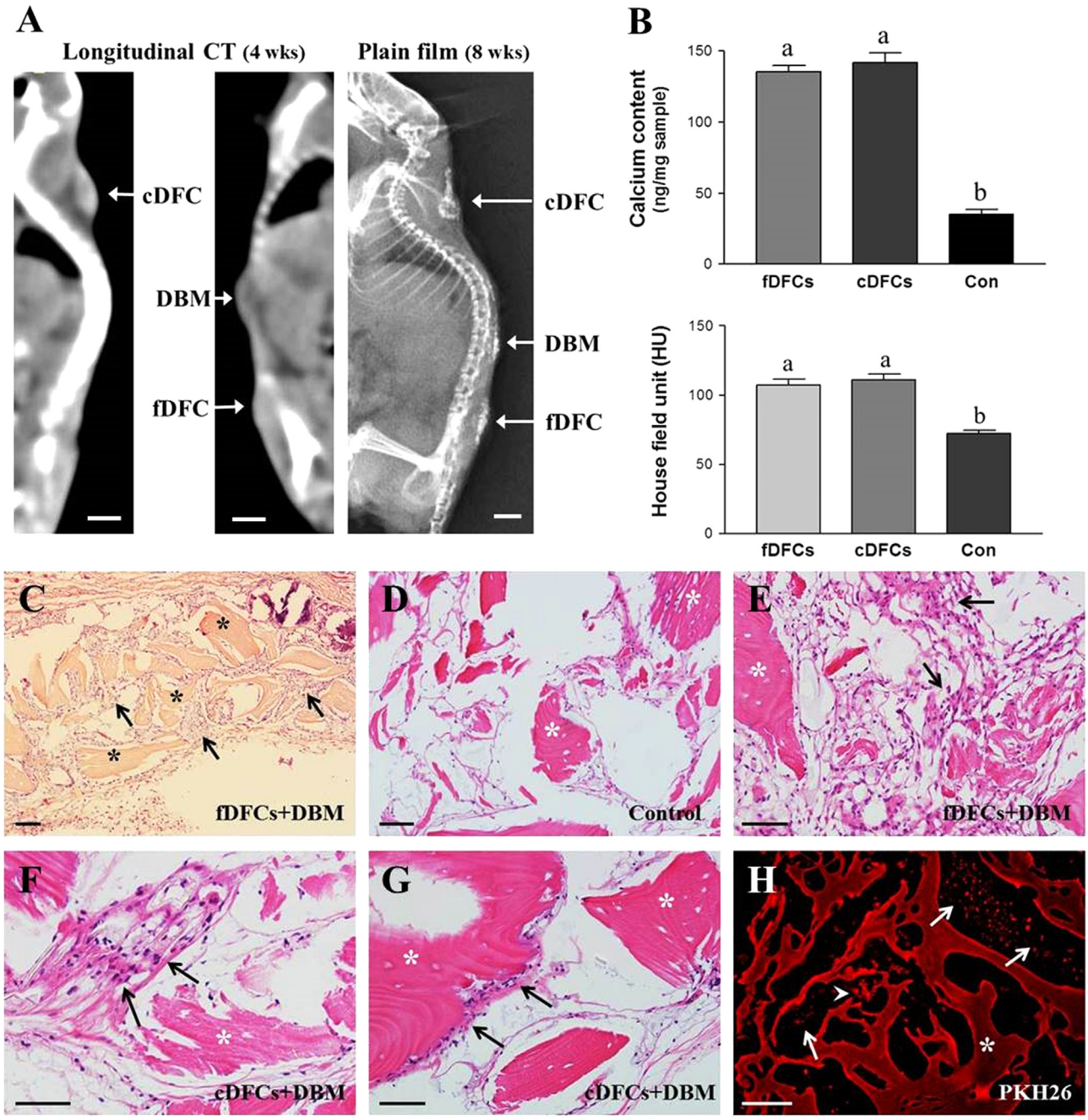

Fig. 5. Radiological and histological analyses of ectopic bone formation in the subcutaneous tissues of mice. (A and B) Transplantation of hDFCs from fresh and cryopreserved dental follicles (fDFCs and cDFCs) showed similar *in vivo* ectopic bone formation potential, and enhanced radiological opacities were observed by digitalized radiological signal intensity analysis compared to that in control sites (DBM-only graft) by CT at 4 weeks post-transplantation. The data represent the mean ± SD of four different experiments. Different letter subscripts denote statistical differences ($p < 0.05$) between groups (A, scale bar = 0.5 cm). (C–H) Histological features of ectopic bone formations at 8 weeks post-implantation (D, DBM-only implanted control site; C & E, fDFC-transplanted site; F and G, cDFC-transplanted site; H, PKH26 expression pattern of cDFC implant site; scale bar = 100 μm). (C) Lower magnification images of the hDFC and DBM-transplanted sites show numerous detectable cells between the transplanted DBM (*) in the subcutaneous tissue of mice. (D-F) The detectable cell number was significantly increased in the hDFC-transplanted sites than in the control sites. Numerous immature fibroblast-like cells (putative pre-osteoblasts, black arrows) were observed in hDFC-grafted sites surrounding DBM scaffolds (*). (G) DBM-lining osteoblasts and osteogenic activity (black arrows) were abundant in the periphery of transplanted DBM (*). (H) White arrows indicate PKH26 expression, cells were labeled at pre-transplantation, around newly generated bone spicules (*). Some transplanted cells are connected to newly generated bone spicules, indicating that transplanted hDFCs were directly converted into osteogenic cells (arrowhead).

bone activity was more frequently observed in hDFC-transplanted sites than in the no graft or DBM-only control sites. In addition, there were no histomorphological differences between fDFC- and cDFC-transplanted groups.

3.3. Analysis of ectopic bone formation in the subcutaneous tissues of mice

In the implanted subcutaneous tissues of experimental mice, ectopic bone formation was observed by CT and conventional radiography (Fig. 5A). The radiological intensity analysis of CT images at 4 weeks post-implantation showed that both of the hDFC-transplanted sites had enhanced radiological opacities compared to the DBM-only grafted control sites (Fig. 5A and B). This finding correlated with that of a previous study (Park et al., 2012). Interestingly, on plain film at 8 weeks post-implantation, the radiological opacity was significantly increased in all implanted sites; however, the hDFC-transplanted sites showed much wider ectopic bone formation than the control sites (Fig. 5A). The total calcium content of the *in vivo* specimens was calculated relative to the total tissue sample (in ng/mg), and the mean values for the fDFCs, cDFCs, and control sites were 135.4 ± 7.8, 141.7 ± 12.3, and 35.2 ± 5.8, respectively (Fig. 5B). Both the fDFC- and cDFC-grafted specimens showed significantly higher calcium content ($p < 0.05$) than the control specimens.

Lower magnification H&E staining showed that all materials implanted in subcutaneous tissues of experimental mice were well preserved (Fig. 5C). The DBM-only grafted control sites showed remarkably less cell density than the two hDFC-grafted sites (Fig. 5D). Higher magnification images of fDFC- and cDFC-transplanted sites showed similar histological morphologies and the same detectable cell numbers (Fig. 5E–G). Evidence of new bone activity, including immature fibroblast-like cells (putative pre-osteoblasts), trabecular lining osteoblasts, and entrapped osteocytes in the new bones, was abundant in the hDFC-transplanted sites (Fig. 5E–G). Fluorescence microscopy of tissue specimens at 8 weeks post-implantation showed pre-labeled PKH26-positive cells in the hDFC-implanted sites, indicating that the transplanted hDFCs were preserved and proliferated *in vivo* (Fig. 5H).

3.4. IHC analysis of OC and VEGF in the newly generated bone of mice and miniature pigs

Expression of OC and VEGF in the ectopic bone of mice and the mandibular defects of miniature pigs was evaluated by IHC. OC and VEGF signals were strong in the hDFC-transplanted sites of the two experimental animals. In particular, strong OC staining was observed in the DBM-lining osteoblasts and fibroblast-like putative pre-osteoblasts in both animal specimens (Fig. 6A and B). In addition, strong VEGF signals were also detected in the osteogenic cells, DBM-lining osteoblasts, and pre-osteoblasts in the ectopic bone of the subcutaneous tissue in mice (Fig. 6C). In miniature pigs, strong VEGF staining was detected in newly generated vascular vessels and blood cells in interstitial tissues between the newly generated bones (Fig. 6D). Semiquantitative analysis of the immunostaining intensities of OC and VEGF in the ectopic bone tissues of mice showed similar expression levels in the fDFC- and cDFC-transplanted sites, and the staining intensity in the hDFC-transplanted groups tended to be higher than that in the control groups; however, there was no statistically significant difference ($p > 0.05$).

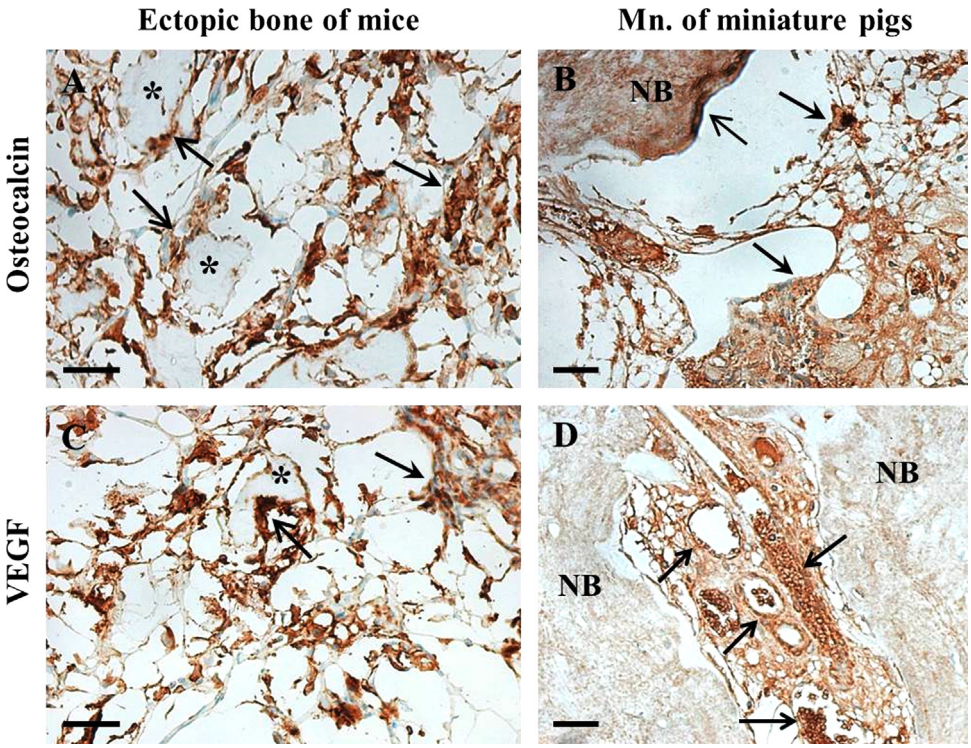

Fig. 6. Immunohistochemical analysis of OC and VEGF in the hDFC and DBM-transplanted subcutaneous tissues of mice (A and C) and mandibular defects (Mn.) of miniature pigs (B and D) (A & B: osteocalcin expression; C and D: VEGF expression; scale bar = 50 μm). (A and B) Strong OC staining was detected in the hDFC-transplanted sites of both animal specimens. Especially, the expression of OC was stronger in osteogenic cells, such as the DBM (*)- and new bone (NB)-lining osteoblasts (open arrows) and fibroblast-like putative pre-osteoblasts (closed arrows). (C) VEGF staining was also strong in the osteogenic cells in the ectopic bone of mice, and the open arrows and closed arrows indicate the DBM (*)-lining osteoblasts and pre-osteoblasts, respectively. (D) In miniature pigs, the VEGF signal was strong in the newly generated vascular vessels and blood cells in the interstitial tissues between the newly generated bones (NB).

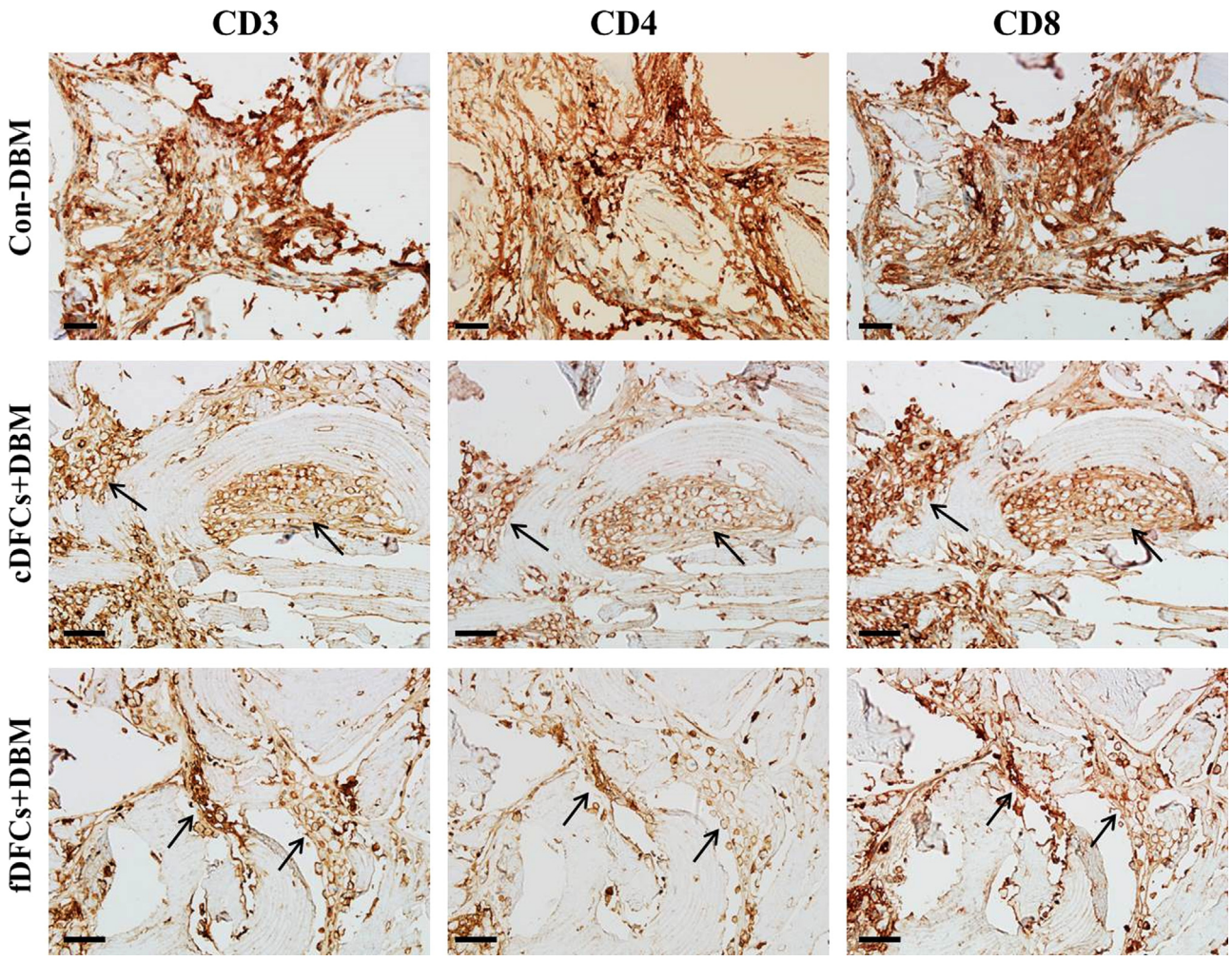

Fig. 7. Immunohistochemical expression of the T-cell markers CD3, CD4, and CD8 in the ectopic bone tissues of mice (scale bar = 50 μm). All three T-cell markers were detected on the cell membrane (arrows). In the DBM-only implanted control sites, strong expression of CD3, CD4, and CD8 was detected. In the serial sections of DFC-transplanted sites, CD8 was strongly expressed, similar to that observed in control specimens. However, CD3 and CD4 expression in the DFC-transplanted sites was lower, and was scored as moderate and weak, respectively. Specifically, CD4 expression in the hDFC-transplanted specimens was significantly different from that in the control specimens (shown in Table 2; $p < 0.05$).

3.5. Analysis of CD3, CD4, and CD8 in the subcutaneous ectopic bone formation sites of mice

IHC analysis of the T-cell markers CD3, CD4, and CD8 showed expression of these proteins on the cell membrane at each implant site (Fig. 7). In the DBM-only grafted control sites, all marker proteins were strongly expressed in the tissues surrounding the implanted DBM scaffolds. In the serial sections of the two hDFC-transplanted sites, CD8 expression was relatively high, similar to that in the control site. However, CD3 and CD4 expression in hDFC-transplanted sites were lower, and were classified as moderate and weak, respectively. CD4 expression in the hDFC-transplanted specimens was significantly lower than that in control specimens ($p < 0.05$; Fig. 7 and Table 2).

4. Discussion

There is an immense need for suitable MSC sources that not only have the potency to differentiate into different cell lineages *in vitro* but also can be efficiently applied to generate the desired output irrespective of whether they are fresh or cryopreserved. The present study showed that both fresh and cryopreserved hDFCs have immunomodulatory characteristics and can be used as a valuable stem cell source in regenerative medicine. Dental tissue can be obtained at relatively late ages compared to other stem cell sources, such as placenta or umbilical cord and blood (Takahashi et al., 2015). Unlike MSCs from bony tissue, such as BMSCs, dental tissue-derived MSCs are considered to be more committed in terms of their potential for differentiation due to a lack of continuous remodeling in dental tissue (Huang et al., 2009). In previous studies, hDFCs from immature wisdom teeth were reported to possess strong mesenchymal characteristics and showed similar or superior *in vitro* and *in vivo* osteogenic differentiation potential compared to that of BMSCs (Park et al., 2012; Takahashi et al., 2015). The dental follicle is an ectomesenchymal tissue that surrounds the developing tooth and possesses abundant progenitors of osteoblasts in alveolar bone, fibroblasts in the periodontal ligament, and cementoblasts in the root cementum (Morsczeck et al., 2009; Park et al., 2012). hDFCs also show constant expression of osteoblast-specific transcription factors and strong mineralization as well as increased expression of osteogenic markers during osteogenic differentiation (Morsczeck et al., 2009; Vollkommer et al., 2015). These results suggest that hDFCs have strong potential for osteogenic differentiation, indicating that they can be used as an excellent source of stem cells for bone tissue engineering (Park et al., 2012; Vollkommer et al., 2015; Takahashi et al., 2015).

In our previous work, we developed a new cryopreservation method for human dental follicle tissue that could be used as a source of autologous stem cells (Park et al., 2014). For clinical application, stem cells cryopreserved for a long period with dimethyl sulfoxide (DMSO) and FBS showed frequent cell damage, contamination, and genetic variation caused by cryoprotectant toxicity or cell dehydration (Rowley et al., 2003; Ock and Rho, 2011; Park et al., 2014). In contrast, long-term cryopreservation of the stem cell source, untreated tissue itself, could be safer and more economical for use in the future. In the present study, the *in vivo* osteogenic potential of MSCs from cryopreserved human dental follicles (cDFCs) was evaluated and compared to that of MSCs from fresh dental follicles (fDFCs). The results of this study showed that fDFCs and cDFCs possessed the same enhanced osteogenic potential after *in vivo* transplantation into experimental animal models, including mandibular bone defects in miniature pigs and ectopic bone formation in the subcutaneous tissue of mice. Interestingly, the hDFC-transplanted sites in mandibular defects of miniature pigs showed new bone formation in excess of the original defect at 8 weeks post-implantation. CT at 4 weeks post-transplantation showed new bone generation not only within the bone defects but also in the muscle layers surrounding the defects (Fig. 3A). Since no overlaying membrane, which is usually applied for guided bone regeneration, was used to cover the graft materials in this experiment, some of the transplanted cells and scaffold might have extravasated from the defects and formed new bone in the muscle layers. However, compared to the DBM-only grafted controls, the cDFC- and fDFC-implanted groups showed quantitatively and qualitatively enhanced bone formation. These results demonstrate that cDFCs and fDFCs possess the same *in vivo* bone regeneration activity, indicating that when hDFCs are appropriately applied, they will enhance *in vivo* bone reconstruction in bony defects. In addition, fDFCs and cDFCs also showed the same *in vivo* ectopic bone formation in the subcutaneous tissues of experimental mice. Sites transplanted with hDFCs and DBM scaffold showed stronger intensities than DBM-only grafted control sites, similar to that reported in a previous study (Park et al., 2012).

To evaluate the immune response following *in vivo* transplantation of hDFCs, tissue specimens from the ectopic bone generation sites were analyzed by IHC to evaluate the expression of T-cell-related glycoproteins, including CD3, CD4, and CD8. The results showed decreased expression of CD3 and CD4 in the hDFC-transplanted specimens compared to that in non-cell-implanted control specimens. Interestingly, CD4 expression was significantly lower in hDFC-transplanted sites than in control sites. CD3 is a T-cell co-receptor that is present during all stages of T-cell development; therefore, it is a useful IHC marker for pan-T cells in tissue sections (Mason et al., 1989). CD4 is a glycoprotein found on the surface of immune cells, including T-helper cells, monocytes, macrophages, and dendritic cells (Ansari-Lari et al., 1996). $CD4^+$ T-cells are usually divided into regulatory T-cells (Treg) and conventional T-helper cells, and 6–9% of $CD4^+$ T-cells belongs to the Treg lineage (Corthay, 2009; Dwivedi et al., 2013; Peterson, 2012). Some studies have demonstrated upregulation of $CD4^+$ cells after *in vivo* MSC transplantation; however, these $CD4^+$ T cells were Treg cells ($CD4^+/CD25^+$) (Kuo et al., 2012; Yamaza et al., 2010; Zhao et al., 2015). In contrast, another study using immunomodulator-treated animals showed decreased CD4 expression by IHC analysis (Lappin and Black, 2003). Moreover, a recent study showed that allogenic MSCs mediated the suppression of $CD4^+$ T-cell proliferation (Bloom et al., 2015). Similar to the present study, *in vivo* hDFC-transplanted sites showed lower expression of CD4 than non-cell-transplanted control sites. Since $CD4^+$ Tregs are not an abundant subset of the $CD4^+$ T-cell population (6–9%), most $CD4^+$ cells are considered T-helpers. Therefore, the lower CD4 expression observed in the hDFC-transplanted tissues is indicative of the decreased activity and reduced number of T-helper cells. In addition, CD4 directly interacts with MHC II molecules on the surface of antigen-presenting cells (Fooksman, 2014). Interestingly, FACS analysis after passage 3 showed that MHC II expression in both types of hDFCs was extremely low in the present study. Moreover, strong expression of CD119, the interferon-γ receptor (IFN-γR), was detected in both fresh and cryopreserved hDFCs. CD119 has been reported as a marker of MSC immunomodulation because most of the inhibitory effects of MSCs on T-cell proliferation require IFN-γ, a pro-inflammatory cytokine (Krampera et al., 2006, 2013). IFN-γ is considered as the first key licensing agent for the suppression function of MSCs, and it augments the immunosuppression of MSCs across species (Krampera et al., 2013). Taken together, these *in vitro* and *in vivo* results indicate that hDFCs possess immunomodulatory activity that is mediated by inhibition of CD4 and MHC II expression, which coincides with suppression of the T-helper cell-mediated adaptive immune response (Ferrante, 2013; Fooksman, 2014).

In support of the present results, several studies have previously reported that MSCs derived from various adult tissues, such as bone marrow, fat, umbilical cord, and dental tissue, possess immunomodulatory and anti-inflammatory effects (Duffy et al., 2011; Le Blanc and Ringdén, 2006; Soleymaninejadian et al., 2012; Yamaza et al., 2010). Although there are many complicated reactions related to the immunomodulation of MSCs, transplantation of MSCs directly or indirectly inhibited disease-associated T-helper cells, reduced cytotoxic lymphocytes, and increased Treg cells (Duffy et al., 2011; Rahimzadeh et al., 2014; Yamaza et al., 2010). Various cytokines and growth factors from undifferentiated MSCs may also play a role in MSC-facilitated immunomodulation (Soleymaninejadian et al., 2012). The immunomodulatory effects of MSCs make them a potentially valuable therapeutic agent against severe autoimmune diseases and graft-versus-host disease (Kuo et al., 2012; Zhao et al., 2015).

In the present study, undifferentiated hDFCs from fresh and cryopreserved dental follicles showed similar MSCs characteristics, with low MHC II expression and high CD119 expression *in vitro*. Moreover, the two types of hDFCs showed identical *in vivo* osteogenic activities, and similar decreased CD4 expression was observed in the hDFC-transplanted tissues. These results demonstrate that hDFCs from fresh and cryopreserved dental follicles possess the same osteogenic differentiation potential and immunomodulatory properties, resulting in inhibition of CD4, MHC II, and the T-helper cell-mediated adaptive immune response, which underscores the usefulness of hDFCs in the field of bone tissue regeneration. The present study also demonstrated that the stemness of long-term preserved dental follicle tissues from extracted wisdom teeth can be restored, and they can be used as an excellent autologous or allogenic stem cell source for tissue engineering or as a therapeutic agent for autoimmune diseases.

Conflict of interest

The authors have declared that there is no conflict of interests.

Acknowledgment

This work was supported by the National Research Foundation of Korea (NRF) Grant funded by the Korean Government (NRF-2014R1A1A2058807) and Gyeongsang National University Hospital Research Foundation Grant (GNUHBIF-2014-0006).

References

Ansari-Lari, M.A., Muzny, D.M., Lu, J., Lu, F., Lilley, C.E., Spanos, S., Malley, T., Gibbs, R.A., 1996. A gene-rich cluster between the CD4 and triosephosphate isomerase genes at human chromosome 12p13. Genome Res. 6, 314–326.

Bloom, D.D., Centanni, J.M., Bhatia, N., Emler, C.A., Drier, D., Leverson, G.E., McKenna Jr., D.H., Gee, A.P., Lindblad, R., Hei, D.J., Hematti, P., 2015. A reproducible immunopotency assay to measure mesenchymal stromal cell-mediated T-cell suppression. Cytotherapy 17, 140–151.

Chao, Y.H., Wu, H.P., Wu, K.H., Tsai, Y.G., Peng, C.T., Lin, K.C., Chao, W.R., Lee, M.S., Fu, Y.C., 2014. An increase in CD3+CD4+CD25+ regulatory T cells after administration of umbilical cord-derived mesenchymal stem cells during sepsis. PLoS One 9, e110338.

Corthay, A., 2009. How do regulatory T cells work? Scand. J. Immunol. 70, 326–336.

Duffy, M.M., Ritter, T., Ceredig, R., Griffin, M.D., 2011. Mesenchymal stem cell effects on T-cell effector pathways. Stem cell Res. Ther. 2, 34.

Dwivedi, M., Laddha, N.C., Arora, P., Marfatia, Y.S., Begum, R., 2013. Decreased regulatory T-cells and CD4(+) /CD8(+) ratio correlate with disease onset and progression in patients with generalized vitiligo. Pigment Cell Melanoma Res. 26, 586–591.

Ferrante, A., 2013. For many but not for all: how the conformational flexibility of the peptide/MHCII complex shapes epitope selection. Immunol. Res. 56, 85–95.

Fooksman, D.R., 2014. Organizing MHC class II presentation. Front. Immunol. 5, 158.

Huang, G.T., Gronthos, S., Shi, S., 2009. Mesenchymal stem cells derived from dental tissues vs. those from other sources: their biology and role in regenerative medicine. J. Dent. Res. 88, 792–806.

Kang, E.J., Byun, J.H., Choi, Y.J., Maeng, G.H., Lee, S.L., Kang, D.H., Lee, J.S., Rho, G.J., Park, B.W., 2010. In vitro and in vivo osteogenesis of porcine skin-derived mesenchymal stem cell-like cells with a demineralized bone and fibrin glue scaffold. Tissue Eng. Part A 16, 815–827.

Krampera, M., Cosmi, L., Angeli, R., Pasini, A., Liotta, F., Andreini, A., Santarlasci, V., Mazzinghi, B., Pizzolo, G., Vinante, F., Romagnani, P., Maggi, E., Romagnani, S., Annunziato, F., 2006. Role for interferon-γ in the immunomodulatory activity of human bone marrow mesenchymal stem cells. Stem Cells 24, 386–398.

Krampera, M., Galipeau, J., Shi, Y., Tarte, K., Sensebe, L., 2013. Immunological characterization of multipotent mesenchymal stromal cells—The international Society for Cellular Therapy (ISCT) working proposal. Cytotherapy 15, 1054–1061.

Kuo, Y.R., Chen, C.C., Goto, S., Huang, Y.T., Wang, C.T., Tsai, C.C., Chen, C.L., 2012. Immunomodulatory effects of bone marrow-derived mesenchymal stem cells in a swine hemi-facial allotransplantation model. PLoS One 7, e35459.

Lappin, P.B., Black, L.E., 2003. Immune modulator studies in primates: the utility of flow cytometry and immunohistochemistry in the identification and characterization of immunotoxicity. Toxicol. Pathol. 31 (suppl), 111–118.

Le Blanc, K., Ringdén, O., 2006. Mesenchymal stem cells: properties and role in clinical bone marrow transplantation. Curr. Opin. Immunol. 18, 586–591.

Mason, D.Y., Cordell, J., Brown, M., Pallesen, G., Ralfkiaer, E., Rothbard, J., Crumpton, M., Gatter, K.C., 1989. Detection of T cells in paraffin wax embedded tissue using antibodies against a peptide sequence from the CD3 antigen. J. Clin. Pathol. 42, 1194–1200.

Morsczeck, C., Schmalz, G., Reichert, T.E., Völlner, F., Saugspier, M., Viale-Bouroncle, S., Driemel, O., 2009. Gene expression profiles of dental follicle cells before and after osteogenic differentiation in vitro. Clin. Oral Investig. 13, 383–391.

Ock, S.A., Rho, G.J., 2011. Effect of dimethyl sulfoxide (DMSO) on cryopreservation of porcine mesenchymal stem cells (pMSCs). Cell Transpl. 20, 1231–1239.

Park, B.W., Kang, E.J., Byun, J.H., Son, M.G., Kim, H.J., Hah, Y.S., Kim, T.H., Kumar, B. M., Ock, S.A., Rho, G.J., 2012. In vitro and in vivo osteogenesis of human mesenchymal stem cells derived from skin, bone marrow and dental follicle tissues. Differentiation 83, 249–259.

Park, B.W., Jang, S.J., Byun, J.H., Kang, Y.H., Choi, M.J., Park, W.U., Lee, W.J., Rho, G.J., 2014. Cryopreservation of human dental follicle tissue for use as a resource of autologous mesenchymal stem cells. J. Tissue Eng. Regen. Med. . http://dx.doi.org/10.1002/term.1945 [Epub ahead of print]

Peterson, R.A., 2012. Regulatory T-cells: diverse phenotypes integral to immune homeostasis and suppression. Toxicol. Pathol. 40, 186–204.

Rahimzadeh, A., Mirakabad, F., Movasaghpour, A., Shamsasenjan, K., Kariminekoo, S., Talebi, M., Shekari, A., Zeighamian, V., Gandomkar Ghalhar, M., Akbarzadeh, A., 2014. Biotechnological and biomedical applications of mesenchymal stem cells as a therapeutic system. Artif. Cells Nanomed. Biotechnol. . http://dx.doi.org/10.3109/ 21691401.2014.968823 [Epub ahead of print]

Rowley, S.D., Feng, Z., Chen, L., Holmberg, L., Heimfeld, S., MacLeod, B., Bensinger, W.I., 2003. A randomized phase III clinical trial of autologous blood stem cell transplantation comparing cryopreservation using dimethylsulfoxide vs dimethylsulfoxide with hydrocyethyl starch. Bone Marrow Transpl. 31, 1043–1051.

Seo, B.M., Sonoyama, W., Yamaza, T., Coppe, C., Kikuiri, T., Akiyama, K., Lee, J.S., Shi, S., 2008. SHED repair critical-size calvarial defects in mice. Oral Dis. 14, 428–434.

Soleymaninejadian, E., Pramanik, K., Samadian, E., 2012. Immunomodulatory properties of mesenchymal stem cells: cytokines and factors. Am. J. Reprod. Immunol. 67, 1–8.

Sui, W., Hou, X., Che, W., Chen, J., Ou, M., Xue, W., Dai, Y., 2013. Hematopoietic and mesenchymal stem cell transplantation for severe and refractory systemic lupus erythematosus. Clin. Immunol. 148, 186–197.

Takahashi, K., Ogura, N., Tomoki, R., Eda, T., Okada, H., Kato, R., Iwai, S., Ito, K., Kuyama, K., Kondoh, T., 2015. Applicability of human dental follicle cells to bone regeneration without dexamethasone: an in vivo pilot study. Int. J. Oral Maxillofac. Surg. 44, 664–669.

Vollkommer, T., Gosau, M., Felthaus, O., Reichert, T.E., Morsczeck, C., Götz, W., 2015. Genome-wide gene expression profiles of dental follicle stem cells. Acta Odontol. Scand. 73, 93–100.

Watanabe, M., Ohnishi, Y., Inoue, H., Wato, M., Tanaka, A., Kakudo, K., Nozaki, M., 2014. NANOG expression correlates with differentiation, metastasis and resistance to preoperative adjuvant therapy in oral squamous cell carcinoma. Oncol. Lett. 7, 35–40.

Yamada, Y., Ito, K., Nakamura, S., Ueda, M., Nagasaka, T., 2011. Promising cell-based therapy for bone regeneration using stem cells from deciduous teeth, dental pulp, and bone marrow. Cell Transpl. 20, 1003–1013.

Yamaza, T., Kentaro, A., Chen, C., Liu, Y., Shi, Y., Gronthos, S., Wang, S., Shi, S., 2010. Immunomodulatory properties of stem cells from human exfoliated deciduous teeth. Stem Cell Res. Ther. 1, 5.

Zhao, K., Lou, R., Huang, F., Peng, Y., Jiang, Z., Huang, K., Wu, X., Zhang, Y., Fan, Z., Zhou, H., Liu, C., Xiao, Y., Sun, J., Li, Y., Xiang, P., Liu, Q., 2015. Immunomodulation effects of mesenchymal stromal cells on acute graft-versus-host disease after hematopoietic stem cell transplantation. Biol. Blood Marrow Transpl. 21, 97–104.

Zhuang, Y., Li, D., Fu, J., Shi, Q., Lu, Y., Ju, X., 2015. Comparison of biological properties of umbilical cord-derived mesenchymal stem cells from early and late passage: immunomodulatory ability is enhanced in aged cells. Mol. Med. Rep. 11, 166–174.